

Study of $\text{Co}_x\text{Pt}_{1-x}$ nanoalloy formation mechanism via single-source precursors

E. Yu. Filatov ^{1,2,a)} A. V. Zadesenets,^{1,2} S. V. Komogortsev,³ P. E. Plyusnin,^{1,2} A. A. Chepurov,⁴ and S. V. Korenev^{1,2}

¹Novosibirsk State University, Pirogova str. 2, 630090 Novosibirsk, Russian Federation

²Nikolaev Institute of Inorganic Chemistry SB RAS, Lavrentyev Ave. 3, 630090 Novosibirsk, Russian Federation

³Kirensky Institute of Physics, Federal Research Center KSC SB RAS, Akademgorodok 50, bld. 38, 660036 Krasnoyarsk, Russian Federation

⁴Sobolev Institute of Geology and Mineralogy SB RAS, Koptuyuga Ave.3, 630090 Novosibirsk, Russian Federation

(Received 14 September 2018; accepted 28 January 2019)

This paper is devoted to the study of formation mechanism of metal solid solutions during the thermolysis of single-source precursors in Co–Pt systems with a wide range of superstructural ordering. It is shown that the thermal decomposition of $[\text{Pt}(\text{NH}_3)_4][\text{Co}(\text{C}_2\text{O}_4)_2(\text{H}_2\text{O})_2] \cdot 2\text{H}_2\text{O}$ salt in helium is critically different from that under hydrogen atmospheres. Thermal degradation under the helium atmosphere is followed by a gradual reduction of platinum and cobalt, and at each thermolysis temperature only one phase is present. At 380 °C an equiatomic $\text{Co}_{0.50}\text{Pt}_{0.50}$ solid solution is formed ($a = 3.749$ (4) Å, $Fm\bar{3}m$ space group, $V/Z = 13.17$ Å³, crystallite size: 5–7 nm). When the precursor is decomposed under a hydrogen atmosphere, the process proceeds mainly through the simultaneous reduction of the platinum and cobalt atoms, and at each temperature section two metal phases are present. The formation of the close to equiatomic $\text{Co}_{0.50}\text{Pt}_{0.50}$ solid solution ($a = 3.782$ (4) Å, $Fm\bar{3}m$ space group, $V/Z = 13.52$ Å³, crystallite size: 7–9 nm) occurs at 450 °C. The calculations of crystallite sizes are confirmed by transmission electron microscopy data. © 2019 International Centre for Diffraction Data. [doi:10.1017/S0885715619000162]

Key words: nanoalloy formation, powder diffraction, nanoparticles, cobalt, platinum

I. INTRODUCTION

CoPt alloys with near-equiatomic composition have a very high energy of crystallographic magnetic anisotropy ($K_1 \approx 5 \times 10^7$ erg cm⁻³) and, as a consequence, high hysteresis properties make them attractive for use as nanomagnets (Komogortsev *et al.*, 2012; Komogortsev *et al.*, 2016). Moreover, there are scientific studies in the literature showing the high catalytic activity of this system (Potemkin *et al.*, 2012; Furukawa *et al.*, 2016; Potemkin *et al.*, 2017).

One of the increasingly popular ways of synthesizing nanosized bimetallic particles is the thermolysis of single-source precursors, in particular, double-complex salts (Plyusnin *et al.*, 2015; Asanova *et al.*, 2016; Barry *et al.*, 2016). The use of such precursors for the production of nanosized alloys has several advantages over other methods (Chepurov *et al.*, 2011). These advantages include the comparative simplicity of the procedure, consisting of a one-step reduction of the precursor compound by an external reductant, or as a result of an intramolecular redox reaction, and the homogeneous distribution of the alloy's atomic components over the particle volume as well as the possibility of preparing a catalyst with a uniform distribution of catalytic particles over the carrier's volume.

In this paper the formation mechanism of nanosized equiatomic bimetallic $\text{Co}_{0.50}\text{Pt}_{0.50}$ solid solutions under the thermal decomposition of single-source precursors with the use of *in situ* X-ray diffraction (XRD) was studied.

II. EXPERIMENTAL

A. Preparation of the precursor

In order to obtain equiatomic $\text{Co}_{0.50}\text{Pt}_{0.50}$ nanoalloys, $[\text{Pt}(\text{NH}_3)_4][\text{Co}(\text{C}_2\text{O}_4)_2(\text{H}_2\text{O})_2] \cdot 2\text{H}_2\text{O}$ double-complex salt (DCS) was synthesized and characterized by a set of physico-chemical methods according to the literature data (Zadesenets *et al.*, 2011).

B. Instrumentation

Thermogravimetric analyses were carried out using a TG 209 F1 Iris thermobalance (NETZSCH, Germany). The measurements were performed using Al_2O_3 crucibles in helium flow and in the hydrogen–helium mixture (6.5% vol. H_2 in He) in the temperature range of 30–400 °C at a heating rate of 1–10 K min⁻¹ and a gas flow rate of 60 ml min⁻¹.

Powder XRD studies of thermolysis products of the prepared compound were carried out using a DRON-RM4 diffractometer ($\text{CuK}\alpha$ -radiation, graphite monochromator on the diffracted beam, ambient temperature). The refinement of lattice parameters was performed by the full profile technique applied to full-range diffraction data using the PowderCell

^{a)} Author to whom correspondence should be addressed.

E-mail: decan@niic.nsc.ru

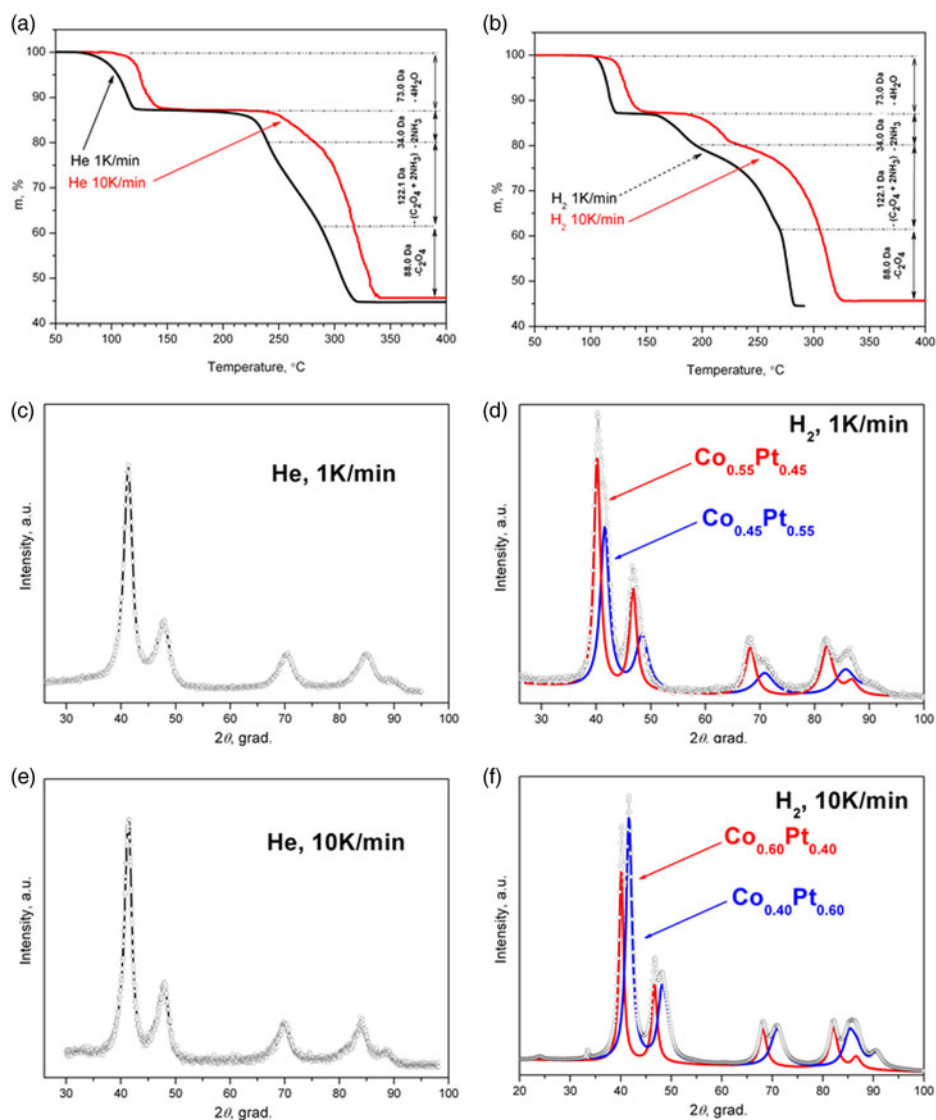


Figure 1. (Color online) Thermogravimetric curves of $[\text{Pt}(\text{NH}_3)_4][\text{Co}(\text{C}_2\text{O}_4)_2(\text{H}_2\text{O})_2] \cdot 2\text{H}_2\text{O}$ DCS decomposition under helium (a) and hydrogen (b) atmospheres at different heating rates (1 and 10 K min^{-1}). Experimental XRD pattern of thermolysis final products under different conditions: helium (c, e) and hydrogen (d, f) atmospheres, 1 (c, d) and 10 K min^{-1} heating rates (e, f); and simulated X-ray powder diffraction patterns for two-phase cases (d, f).

2.4 program (Kraus and Nolze, 2000). The crystallite sizes of the metal phases were determined by the Scherrer equation (WINFIT 1.2.1 (Krumm, 1995)).

Thermal destruction of DCSs under reaction conditions was investigated by *in situ* XRD using an XRK-900 high-temperature reactor chamber (Anton Paar, Austria) mounted on a powder diffractometer of the High Precision Diffraction beamline at the Siberian Synchrotron and the Terahertz Radiation Center and the OD-3M-350 one-coordinate detector (Aulchenko *et al.*, 2009). The detector has 3328 channels covering a 30° 2θ range. The synchrotron radiation wavelength was adjusted to $\lambda = 1.640 \text{ \AA}$. The XRD patterns were recorded for a time of 60 s. The DCS samples were loaded into an open holder allowing the gas (helium or hydrogen) to pass through the entire volume of the sample, and then the holder was placed into the reactor chamber.

High-resolution transmission electron microscopy (HRTEM) measurements were performed using a JEM-2010 electron microscope (lattice plane resolution 0.14 nm at an

accelerating voltage of 200 kV). Images of periodic structures were analyzed by the Fourier method. Local energy-dispersive X-ray (EDX) analysis was carried out using an EDX spectrometer (EDAX Co.) fitted with a Si (Li) detector with a resolution of 130 eV. The error of the metal particle composition determination typically was 0.05 at.% or higher. The samples for the HRTEM study were prepared on a perforated carbon film mounted on a copper grid.

III. RESULTS AND DISCUSSION

The stage thermolysis mechanism of $[\text{Pt}(\text{NH}_3)_4][\text{Co}(\text{C}_2\text{O}_4)_2(\text{H}_2\text{O})_2] \cdot 2\text{H}_2\text{O}$ in helium and hydrogen at heating rates of 10 K min^{-1} was studied by *ex situ* experiment and described in detail in Zadesenets *et al.* (2011). In this experiment we tried to decrease the final temperature by changing the atmosphere of thermolysis from helium to hydrogen and by varying the heating rate for decreasing the size of nanoalloys.

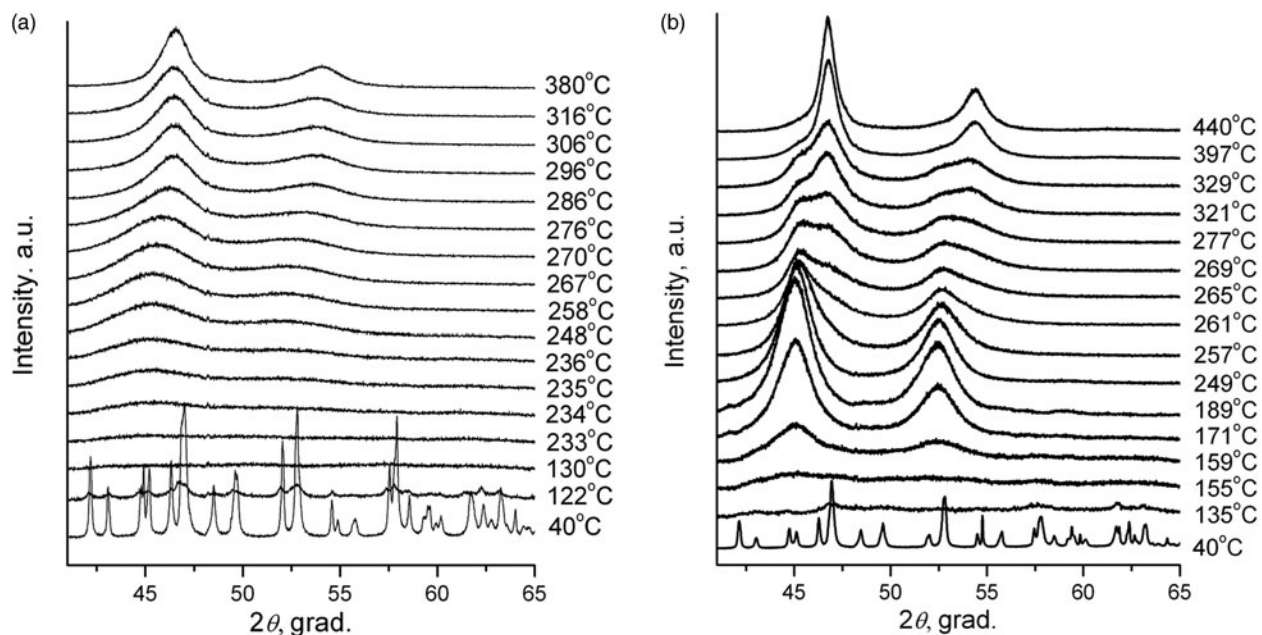


Figure 2. *In situ* XRD patterns of intermediate products of $[\text{Pt}(\text{NH}_3)_4][\text{Co}(\text{C}_2\text{O}_4)_2(\text{H}_2\text{O})_2] \cdot 2\text{H}_2\text{O}$ DCS thermolysis under helium (a) and hydrogen (b) atmospheres.

The shape of the mass loss curve of $[\text{Pt}(\text{NH}_3)_4][\text{Co}(\text{C}_2\text{O}_4)_2(\text{H}_2\text{O})_2] \cdot 2\text{H}_2\text{O}$ under the hydrogen atmosphere is similar to the inert atmosphere (Figure 1). This fact allowed us to state that the stage mechanism of thermolysis under the inert and reducing atmosphere is the same. The differences are manifested only at the temperatures of stage initiation and ending: under a reducing atmosphere, the stage

temperatures are shifted to a lower temperature region. From this fact a logical assumption follows: the lower the temperature of the thermolysis termination, the smaller the particles can be obtained.

However, if we compare thermolysis products under an inert and reducing atmosphere with different heating rates (1 and 10 K min^{-1}), it turns out that in hydrogen, unlike

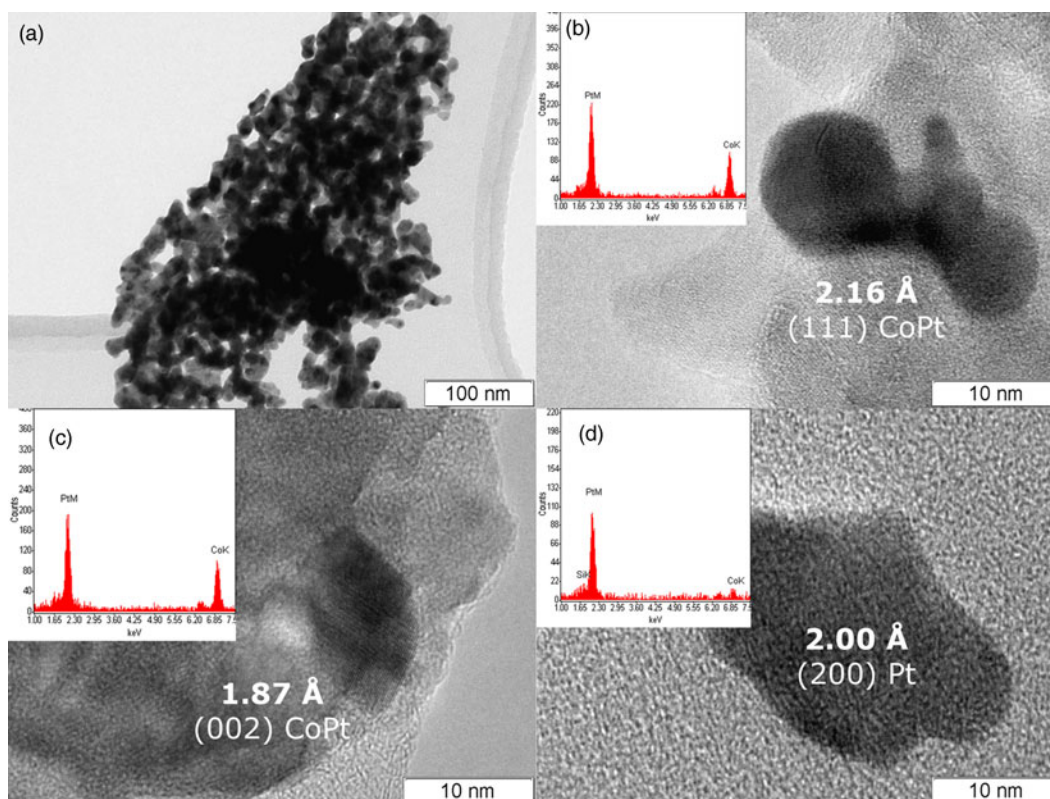


Figure 3. (Color online) TEM photographs of $\text{Co}_{0.5}\text{Pt}_{0.5}$ nanoparticles (a, b, c) and metallic platinum (d) obtained under helium at 380 °C (a, b) and hydrogen at 450 °C (c, d) atmospheres.

helium, it is not possible to obtain a single-phase solid solution under such conditions. To explain this phenomenon, *in situ* XRD experiments for DCS thermolysis were conducted in a high-temperature chamber with a synchrotron radiation source.

As can be seen (Figure 2(a)), during the DCS thermolysis under the helium atmosphere, the diffraction reflexes from the initial complex compound disappear at 130 °C, and the sample becomes amorphous while the uniform background appears on the diffraction pattern. At 234 °C, the separation and crystallization of metallic platinum begins: the intensity of the diffraction peaks increases, and the half-width decreases. When heated above 267 °C, face-centered cubic (fcc) cell diffraction peaks begin to shift toward a high-angle region, which indicates a decrease in the parameters of the unit cell, and, accordingly, the incorporation of metallic cobalt into the platinum structure. At 380 °C the displacement of the cell parameters ceases, which indicates the formation of a final thermolysis product representing a single-phase disordered bimetallic Co_{0.50}Pt_{0.50} solid solution ($a = 3.749(4) \text{ \AA}$, $Fm\text{-}3m$ space group, $V/Z = 13.17 \text{ \AA}^3$, crystallite size: 5–7 nm). The results are confirmed by microscopic data and the EDX spectrum. In the common view of TEM image (Figure 3(a)), it is seen that the product is an agglomerate of nanoparticles with sizes of 7–14 nm. A HRTEM image (Figure 3(b)) demonstrates the polycrystalline structure of nanoparticles. The size of crystalline domains of 6–12 nm coincides with the size of crystallites found from the XRD data. The EDX analysis (inset in Figure 3(b)) suggests the presence of Co and Pt in the same proportion as in the initial precursor. The interplanar distance determined by electron diffraction also indicates the formation of a solid solution CoPt.

The diffraction patterns of the precursor thermolysis products obtained *in situ* under heating under the same conditions but under a hydrogen atmosphere (Figure 2(b)) indicate a significant effect of the hydrogen as a reducing agent in the process of metal reduction. At about 155 °C, as under an inert atmosphere, metallic platinum reflexes appear, the intensity of which increases with increasing temperature, indicating the process of metallic platinum separation. However, at 257 °C additional reflexes appear corresponding to the fcc lattice of the disordered Co_{0.50}Pt_{0.50} solid solution, whose intensity increases with further heating, and the intensity of metallic platinum reflexes decreases. This fact indicates that the separated metallic platinum interacts with the liberating atoms of metallic cobalt to form Co_{0.50}Pt_{0.50} solid solution, bypassing the intermediate stages of the Co_xPt_{1-x} solid solution formation where $x \in [0, 0.5]$. When the temperature reaches 450 °C, the reflexes of metallic platinum disappear completely and only the reflexes of the disordered near-equiatomic cobalt and platinum solid solution are left on the diffraction pattern ($a = 3.782(4) \text{ \AA}$, $Fm\text{-}3m$ space group, $V/Z = 13.52 \text{ \AA}^3$, crystallite size: 7–9 nm at 450 °C). At the same time, the particles of Co_{0.50}Pt_{0.50} solid solution (Figure 3(c)) and a small number of metallic platinum particles of similar size are observed in the HRTEM micrographs (Figure 3(d)). The EDX analysis (inset in Figure 3(c)) suggests the presence of Co and Pt in the same proportion as in the initial precursor or practical pure platinum (inset in Figure 3(d)). The interplanar distance determined by electron diffraction also indicates the formation of a solid solution CoPt or pure Pt.

It should be mentioned the fact that in *ex situ* experiments dehydrated DCS exists in thermolysis products up to a temperature close to the decomposition termination temperature. On the contrary, in *in situ* experiments we pass through amorphization of the DCS.

Thus, the best result for the synthesis of single-phase nanosized particles of Co_{0.50}Pt_{0.50} solid solution is achieved by the thermal decomposition of [Pt(NH₃)₄][Co(C₂O₄)₂(H₂O)₂]·2H₂O under a helium atmosphere at a 10 K min⁻¹ heating rate.

IV. CONCLUSION

The importance of detailed determination of the precursor thermolysis mechanism and the formation of a solid solution is shown, which allows the optimal process parameters to be selected for obtaining the desired product.

[Pt(NH₃)₄][Co(C₂O₄)₂(H₂O)₂]·2H₂O DCS decomposition mechanism is quite complex and depends on regenerative ability of ligands under an inert atmosphere and significant effect of the hydrogen as a reducing agent. The shape of its mass loss curve under the hydrogen atmosphere is similar to that of the inert atmosphere, but the final products of thermolysis are radically different.

Thus, during [Pt(NH₃)₄][Co(C₂O₄)₂(H₂O)₂]·2H₂O DSC thermolysis at relatively low temperature (350 °C) under a hydrogen atmosphere, disordered solid solutions are formed with compositions close to Co_{0.50}Pt_{0.50} and crystallite sizes of 2–4 nm. A single-phase product can be obtained only at a temperature of 450 °C ($a = 3.782(4) \text{ \AA}$, $Fm\text{-}3m$ space group, $V/Z = 13.52 \text{ \AA}^3$, crystallite size: 7–9 nm) or greater.

Under an inert atmosphere, the platinum atoms are successively reduced, followed by cobalt atoms, which are incorporated into the platinum lattice and form Co_xPt_{1-x} solid solution. The process is completed at 380 °C by the formation of Co_{0.50}Pt_{0.50} solid solution ($a = 3.749(4) \text{ \AA}$, $Fm\text{-}3m$ space group, $V/Z = 13.17 \text{ \AA}^3$, crystallite size: 5–7 nm).

ACKNOWLEDGEMENTS

This work was supported by the Russian Foundation for Basic Research (Grant nos. 17-03-00950 and 18-03-00777). Aleksei Chepurov acknowledges support of the state assignment project 0330-2016-0012.

- Asanova, T., Asanov, I., Zadesenets, A., Filatov, E., Plyusnin, P., Gerasimov, E., and Korenev, S. (2016). "Study on thermal decomposition of double complex salt [Pd(NH₃)₄][PtCl₆]." *J. Therm. Anal. Calorim.* **123**(2), 1183–1195.
- Aulchenko, V. M., Evdokov, O. V., Kutovenko, V. D., Pirogov, B. Ya., Sharafutdinov, M. R., Titov, V. M., Tolochko, B. P., Vasiljev, A. V., Zhogin, I. L., and Zhulanov, V. V. (2009). "One-coordinate X-ray detector OD-3M," *Nucl. Instrum. Methods Phys. Res., Sect. A.* **603**, 76–79.
- Barry, M. C., Wei, Z., He, T., Filatov, A. S., and Dikarev, E. V. (2016). "Volatile single-source precursors for the low-temperature preparation of sodium-rare earth metal fluorides," *J. Am. Chem. Soc.* **138**(28), 8883–8887.
- Chepurov, A. I., Sonin, V. M., Chepurov, A. A., Zhimulev, E. I., Tolochko, B. P., and Eliseev, V. S. (2011). "Interaction of diamond with ultrafine Fe powders prepared by different procedures," *Inorg. Mater.* **47**, 864–868.
- Furukawa, S., Ehara, K., and Komatsu, T. (2016). "Unique reaction mechanism of preferential oxidation of CO over intermetallic Pt₃Co catalysts: surface-OH-mediated formation of a bicarbonate intermediate," *Catal. Sci. Technol.* **6**, 1642–1650.

- Komogortsev, S. V., Chizhik, N. A., Filatov, E. Yu., Korenev, S. V., Shubin, Yu. V., Velikanov, D. A., Iskhakov, R. S., and Yurkin, G. Yu. (2012). "Magnetic properties and $L1_0$ phase formation in CoPt nanoparticles," *Solid State Phenom.* **190**, 159–162.
- Komogortsev, S. V., Iskhakov, R. S., Zimin, A. A., Filatov, E. Yu., Korenev, S. V., Shubin, Yu. V., Chizhik, N. A., Yurkin, G. Yu., and Eremin, E. V. (2016). "The exchange interaction effects on magnetic properties of the nanostructured CoPt particles," *J. Magn. Magn. Mater.* **401**, 236–241.
- Kraus, W., and Nolze, G. (2000). *PowderCell 2.4, Program for the Representation and Manipulation of Crystal Structures and Calculation of the Resulting X-ray Powder Patterns* (Federal Institute for Materials Research and Testing, Berlin).
- Krumm, S. (1995). "An interactive windows program for profile fitting and size/strain analysis," *Mater. Sci. Forum* **228–231**, 183–188.
- Plyusnin, P. E., Makotchenko, E. V., Shubin, Y. V., Baidina, I. A., Korolkov, I. V., Sheludyakova, L. A., and Korenev, S. V. (2015). "Synthesis, crystal structures, and characterization of double complex salts $[\text{Au}(\text{en})_2][\text{Rh}(\text{NO}_2)_6] \cdot 2\text{H}_2\text{O}$ and $[\text{Au}(\text{en})_2][\text{Rh}(\text{NO}_2)_6]$," *J. Mol. Struct.* **1100**, 174–179.
- Potemkin, D. I., Filatov, E. Yu., Zadesenets, A. V., Snytnikov, P. V., Shubin, Yu. V., and Sobyenin, V. A. (2012). "Preferential CO oxidation over bimetallic Pt–Co catalysts prepared via double complex salt decomposition," *Chem. Eng. J.* **207–208**, 683–689.
- Potemkin, D. I., Filatov, E. Yu., Zadesenets, A. V., and Sobyenin, V. A. (2017). "CO preferential oxidation on $\text{Pt}_{0.5}\text{Co}_{0.5}$ and Pt–CoOx model catalysts: catalytic performance and *operando* XRD studies," *Catal. Commun.* **100**, 232–236.
- Zadesenets, A., Filatov, E., Plyusnin, P., Baidina, I., Dalezky, V., Shubin, Yu., Korenev, S., and Bogomyakov, A. (2011). "Bimetallic single-source precursors $[\text{M}(\text{NH}_3)_4][\text{Co}(\text{C}_2\text{O}_4)_2(\text{H}_2\text{O})_2] \cdot 2\text{H}_2\text{O}$ ($M = \text{Pd}, \text{Pt}$) for the one run synthesis of CoPd and CoPt magnetic nanoalloys," *Polyhedron* **30**, 1305–1312.